Improving strong lensing models with MAAT

Jose M. Diego

IFCA, Santander, Spain

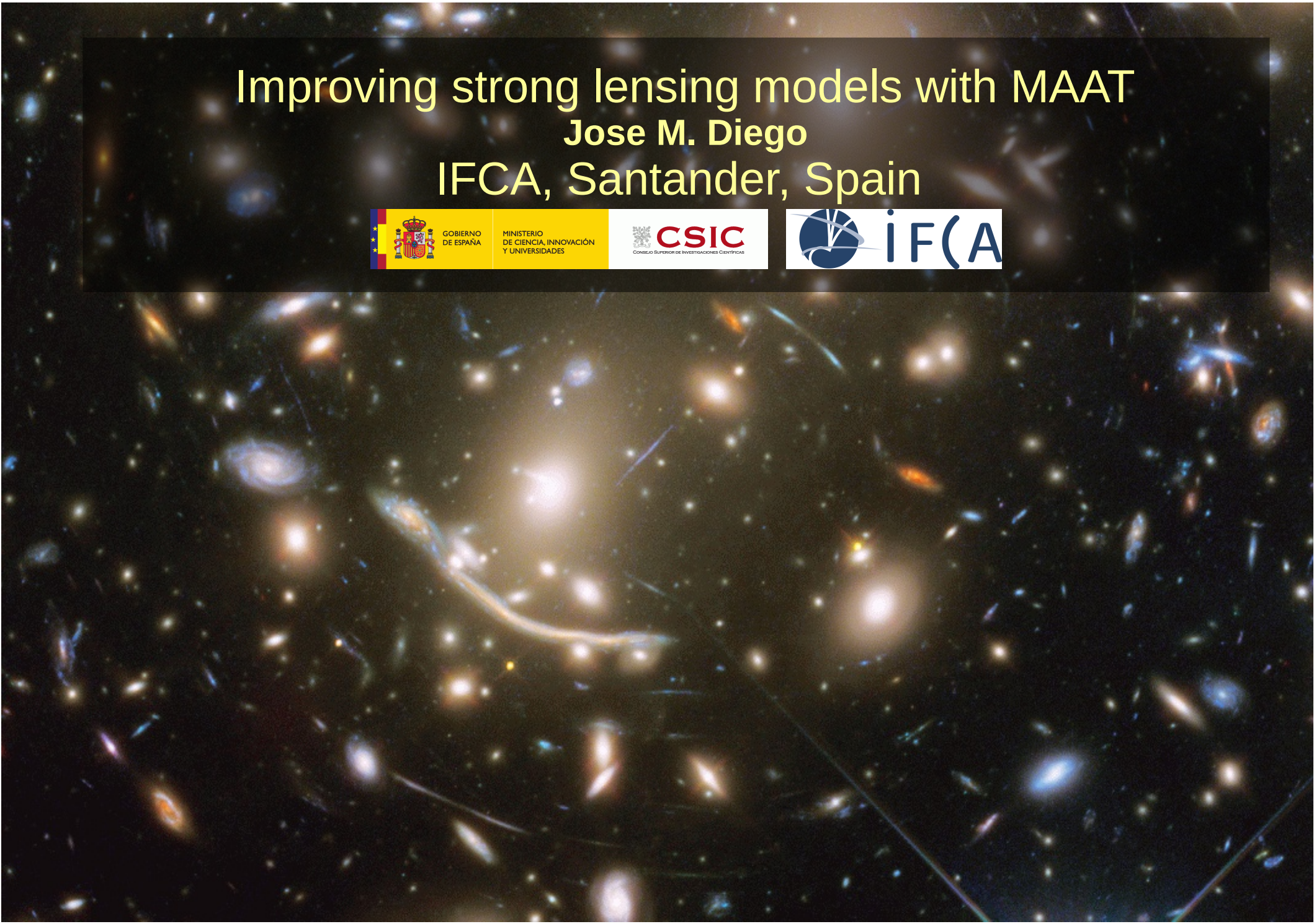

CLASH (25) and RELICS (41) programs provide high resolution HST imaging of >50 lenses. More clusters in other programs.

All together, they have unveiled hundreds of strongly lensed galaxies up to z~10

Magnification factors can reach a few tens, or more than 3 magnitude gain, allowing to study high-z objects in greater detail.

Stark+17
z = 7.733
Lyα 1216Å
[CIII] 1907Å
CIII] 1909Å
detections

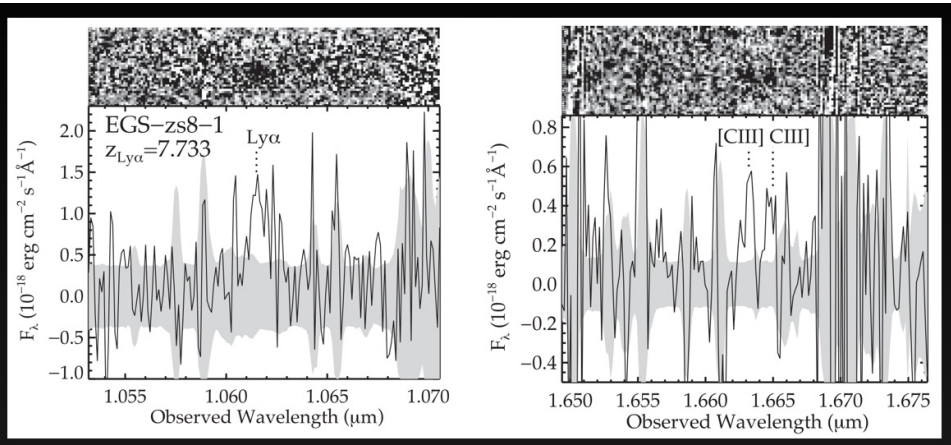

COSMOS
enriched
Pop III?
(HeII 1640Å
detection)
z = 6.604
Sobral+15

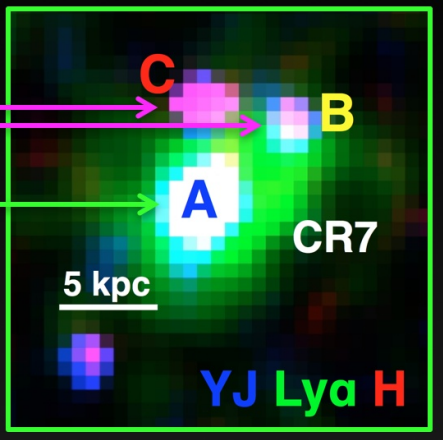

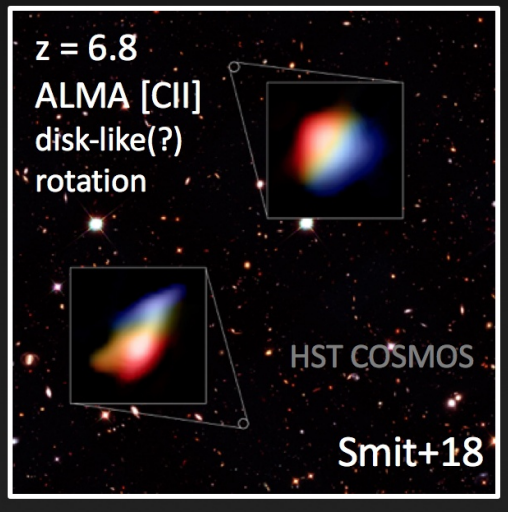

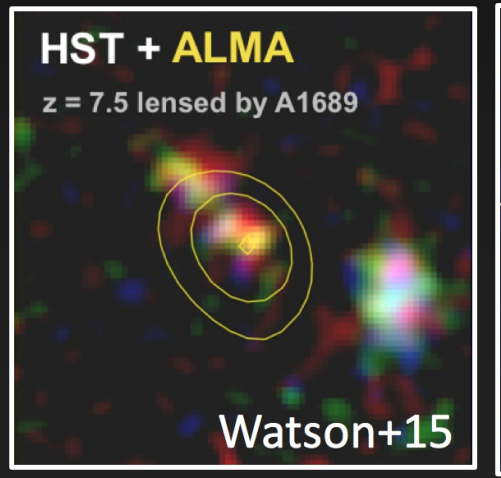

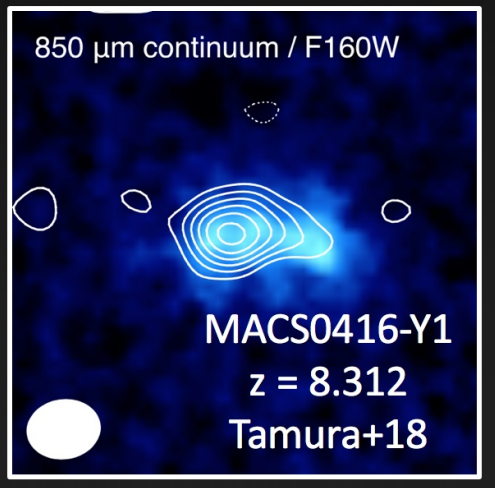

Surprisingly dusty distant galaxies

also see ALMA [OIII] detections in lensed galaxies out to z = 9.11 (Hashimoto+18)

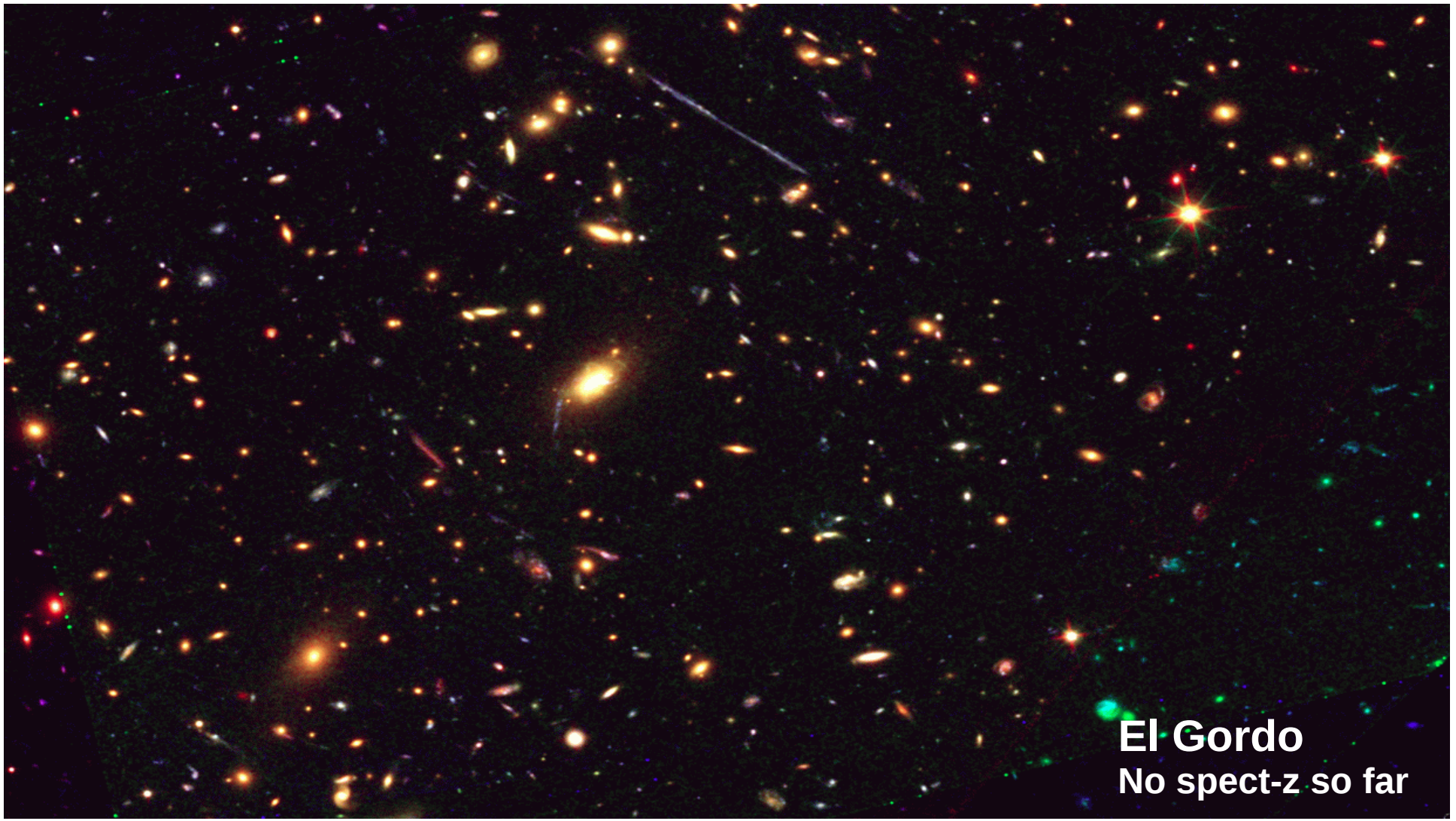

Deep High Resolution images of galaxy clusters often reveal a wealth of strongly lensed galaxies.

Spectroscopic redshifts are needed to properly model the lenses and confirm the lensed systems.

IFU offers the most cost effective way of measuring redshifts of background lensed galaxies.

The Hubble Frontier Fields (HFF)

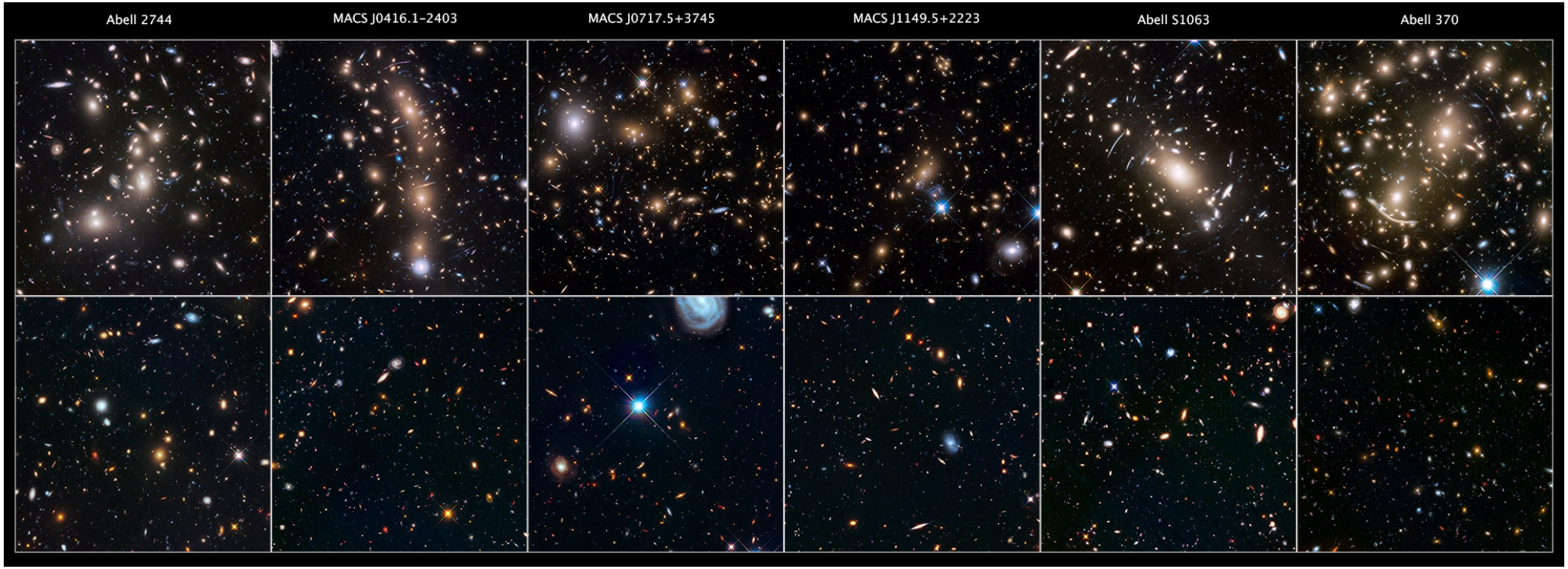

Hundreds of lensed galaxies at high redshift

IFU is the most efficient way of confirming lensed systems, and getting their redshifts

Opportunity to study distant galaxies in detail (~ 2 magnitudes boost)

IFU of HFF clusters

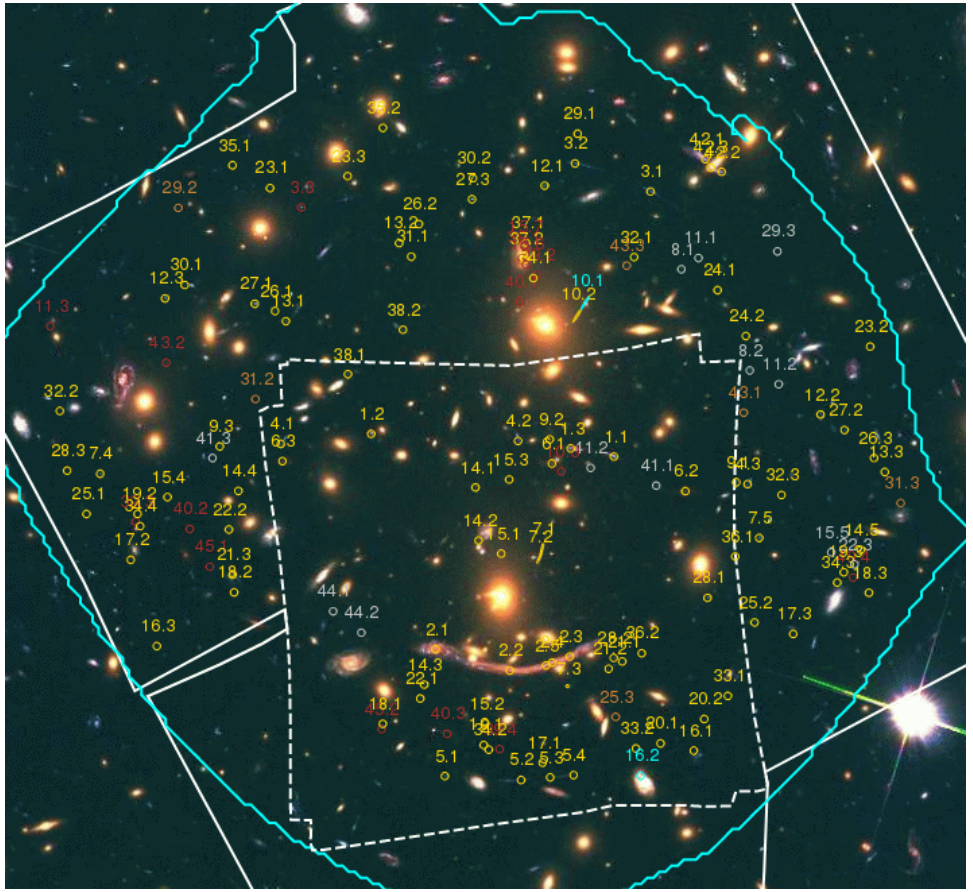

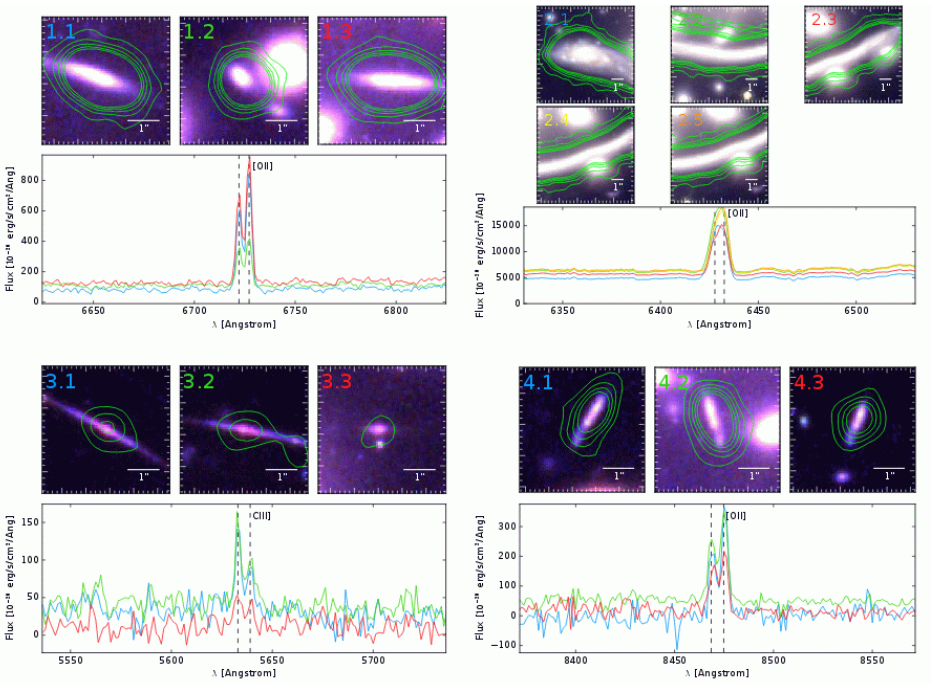

Lagatutta et al. 2019

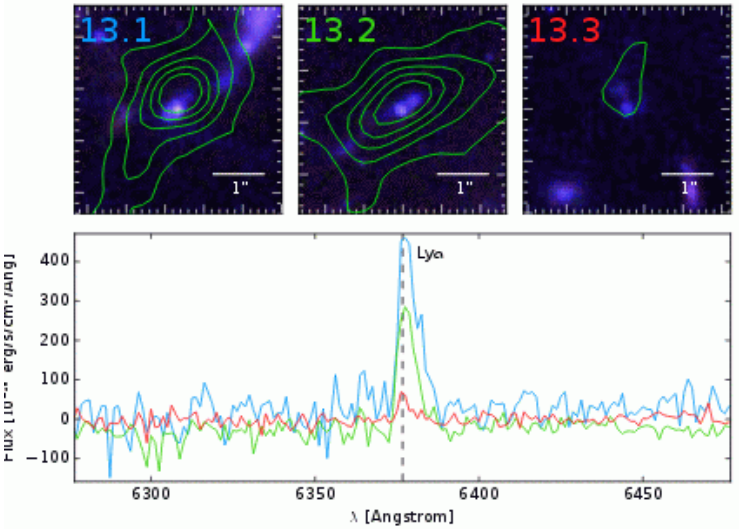

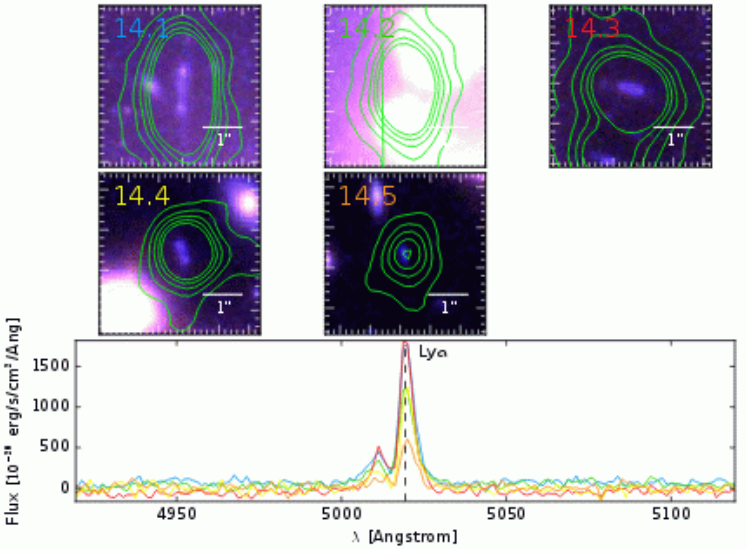

Knot identification with IFU

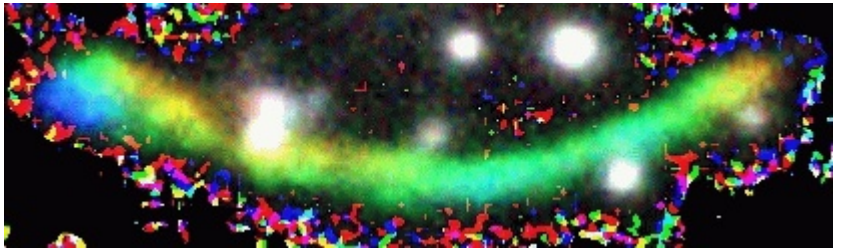

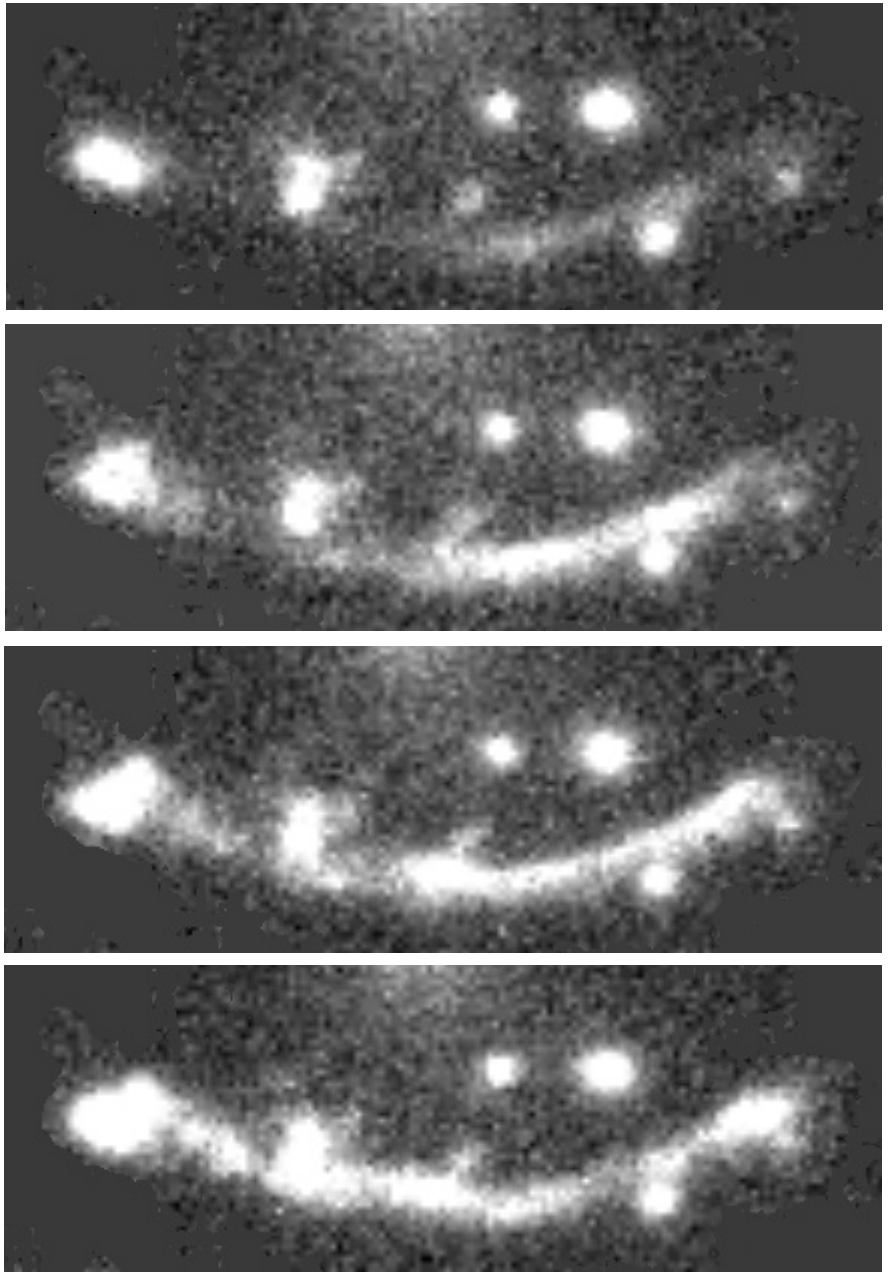

Complementary mass estimates from velocity maps from IFU

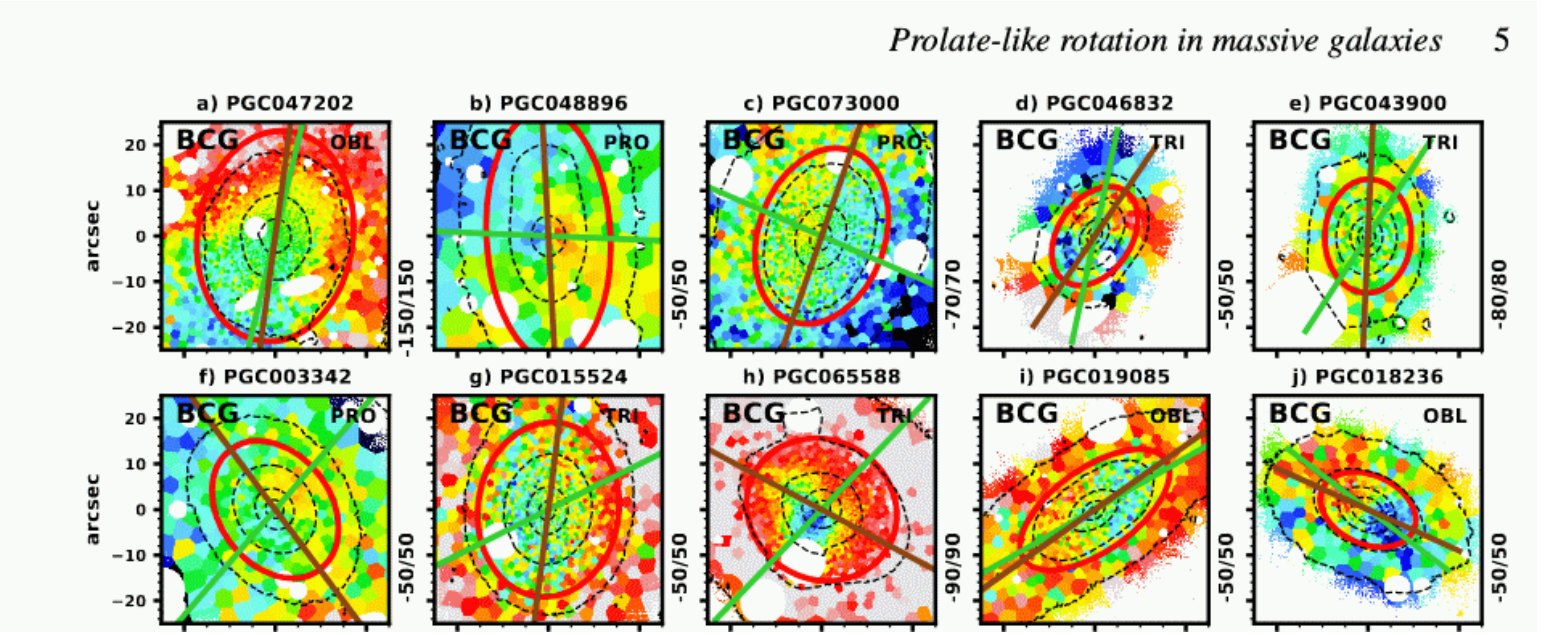

Karman et al. 2015

Krajnovic et al. 2017

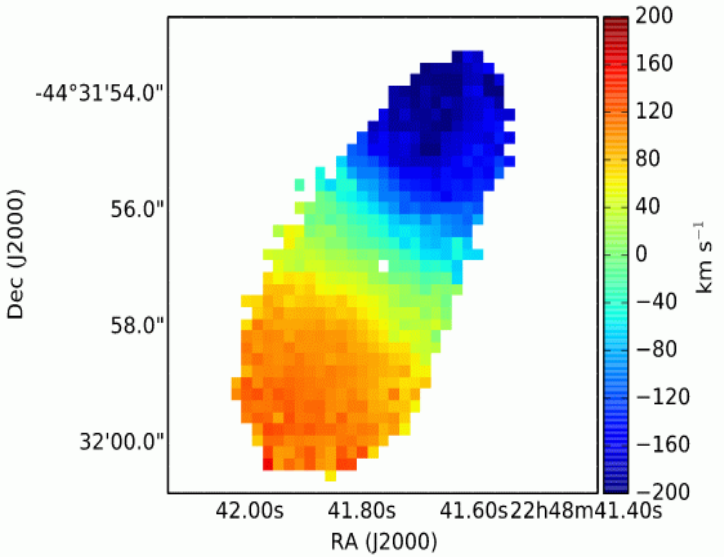

Fig. 7. [O II] velocity map of galaxy 38 at $z = 0.607$. The coordinates are shown on the axes, and the velocity is given for every pixel by its colour. This figure clearly illustrates the power of MUSE for 2D spectroscopy.

Estimating both, the velocity of the central BCG as well as velocity dispersion of the member galaxies provides valuable complementary information to the lensing constraints to improve the lens model.

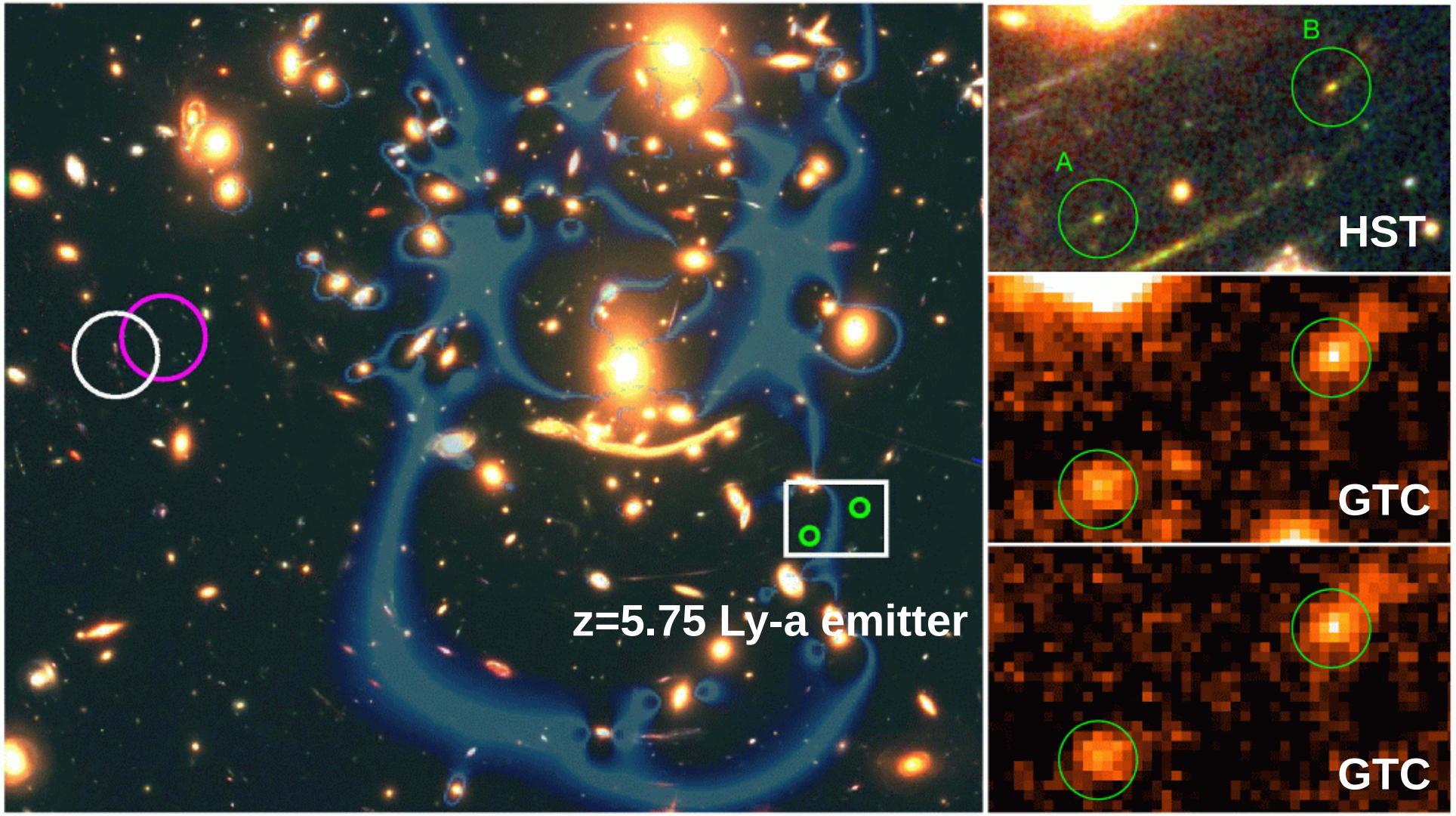

Figure 1. Left: RGB composite image of a 115″ × 100″ region in the central part of the Abell 370 galaxy cluster, obtained by combining HFF frames in the F160W (red), F814W (green), and F435+F606W (blue) filters. The cyan overlay represents the magnification map from the lens model of Diego et al. (2016). The white box encloses counterimages A and B of the $z = 5.75$ LAE A370-L57 (green circles), while the white and pink circles mark the 5″ error circles around the expected position for counterimage C according to the lens models of Diego et al. (2016) and Lagattuta et al. (2017), respectively. Right: enlarged view of the area inside the white box as seen in the RGB composite image (top), SHARDS F823W17 direct image (middle), and F823W17 residual frame after subtraction of a PSF-matched version of the F814W image (bottom). The radius of the green circles is 1″.

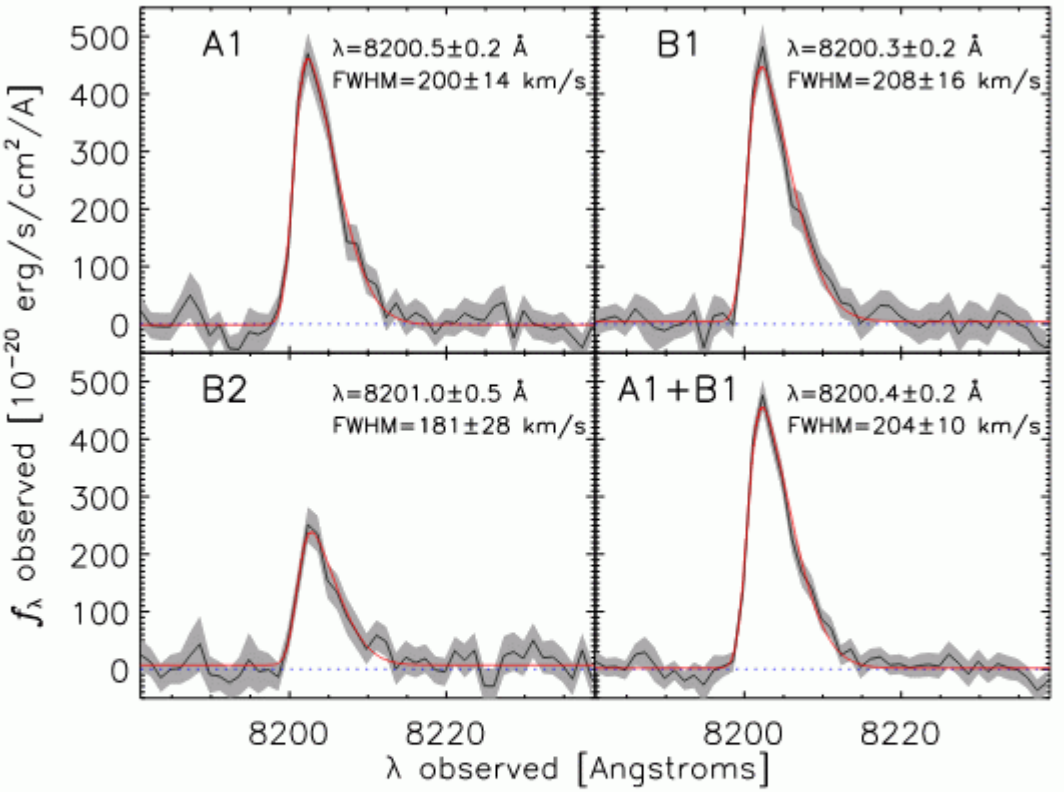

Figure 6. Lyα profiles for sources A1, B1, B2, and the combined spectrum of A1 and B1. Each spectrum is the combination of the three individual spectra extracted on different MUSE data cubes. The shaded area represents the 1σ uncertainties, while the red solid line is the best-fitting model consisting of a half Gaussian convolved with the instrumental profile. The derived peak wavelength and FWHM corrected for instrumental broadening are shown in the upper right corner.

EW~470 Angstrom

A “typical” galaxy responsible of cosmic reionization?

Transients in galaxy clusters offer a unique opportunity to study both the dark matter (warm, PBHs, wave DM, ...) and the cosmological model (time delays).

Accurate characterization of the background source (spectra) is fundamental to reduce the space of parameters and eliminate degeneracies.

Good examples are SNe and magnified stars, including PopIII but also QSO's (variable)

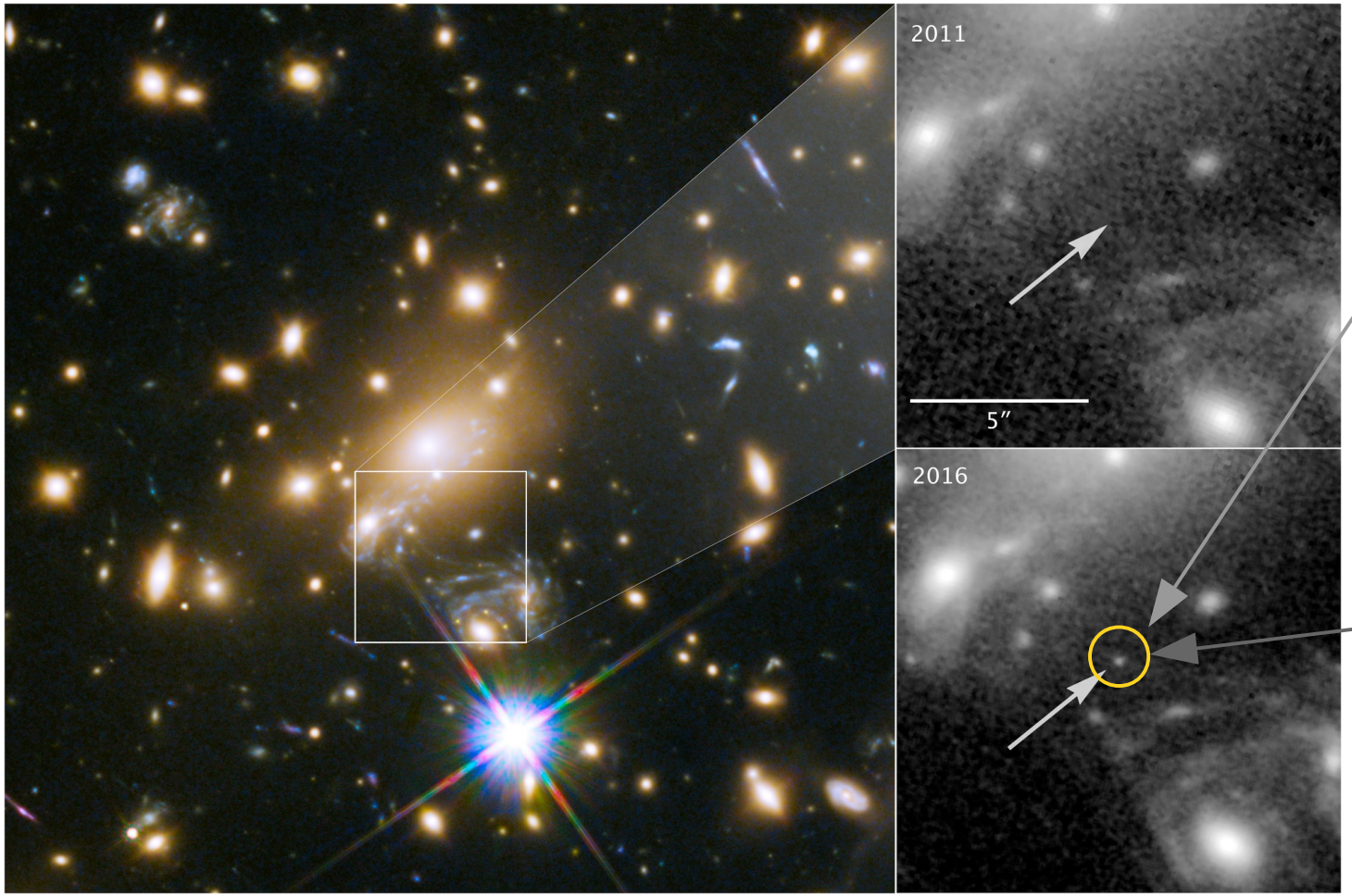

Kelly et al. 2018

Icarus star @ z=1.49

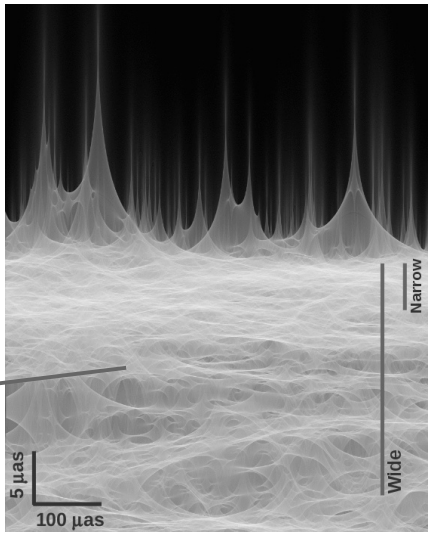

Diego et al. 2018
Diego 2019

Refsdal constraints on H_o

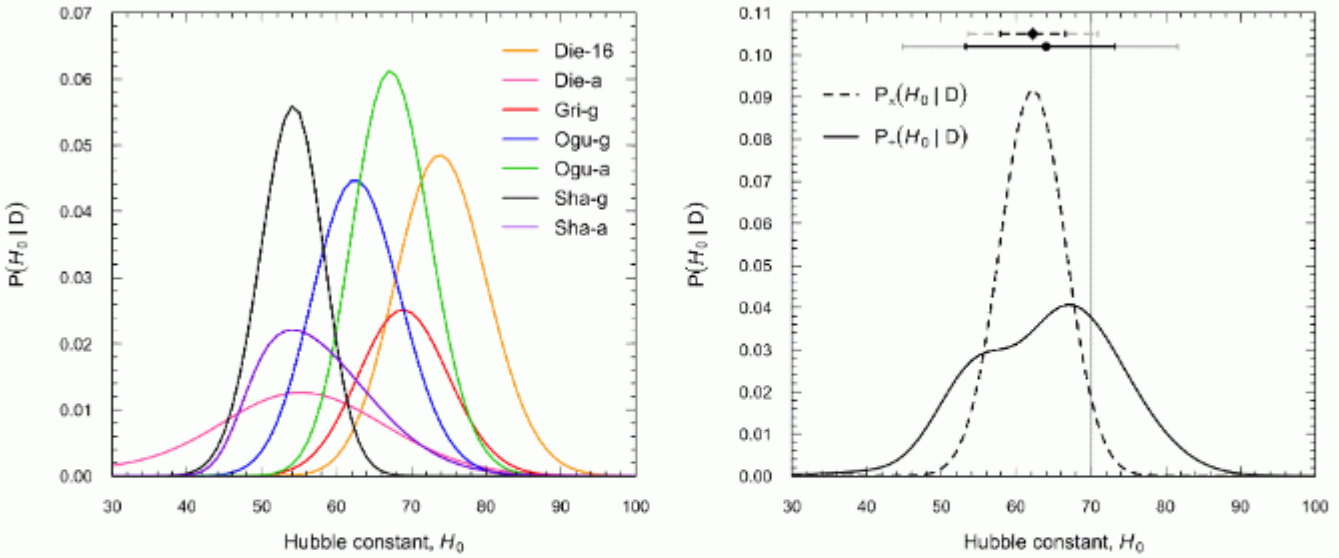

Figure 2: Left-hand panel extracted from [33]: Contribution of each lens model prediction (in different colors) to the posterior $P_+(H_0|D)$ obtained by equation 3. Right-hand panel extracted from [33]: Total posterior $P_\times(H_0|D)$ (dashed line) and $P_+(H_0|D)$ (solid line). Both curves include a systematic uncertainty at the 6% level added at the end in quadrature to the statistical uncertainty. We explicitly show the median, 68% CL (black error bars) and 95% CL (grey error bars) on the top of the figure for both posteriors. The vertical line corresponds to the fiducial $H_0^{\rm fid} = 70$ km s^{-1} Mpc^{-1} assumed in all the lens models.

Vega-Ferrero et al. 2019

Need accurate lens models

Gravitational Lenses in J-PAS

http://archive.cefca.es/catalogues/minijpas-pdr201912

Approx. 5000 sq. degrees in 54 NB filters (plus 3-4 BB filters and 1 MB filter).

Accurate spectroscopic redshifts

Great potential to identify “rare” objects, based on their spectroscopic signature.

Strong lensing with J-PAS

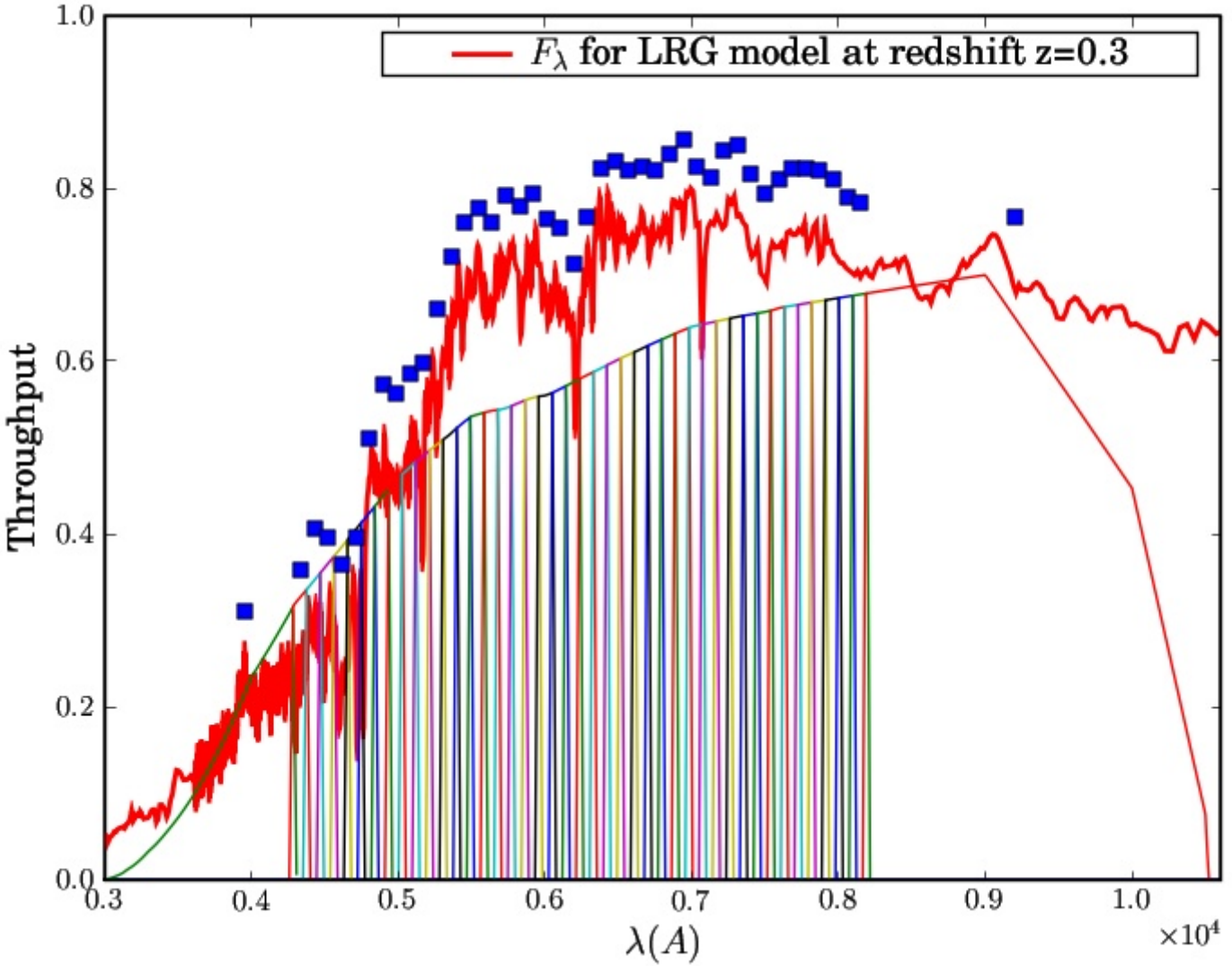

Most lenses will be elliptical galaxies

Most background objects will be at z~2 (SF galaxies with lines).

Many lens systems will appear as a superposition of two spectra (LRG+SF galaxy)

J-PAS specially well suited to discover gravitationally lensed high-z QSO

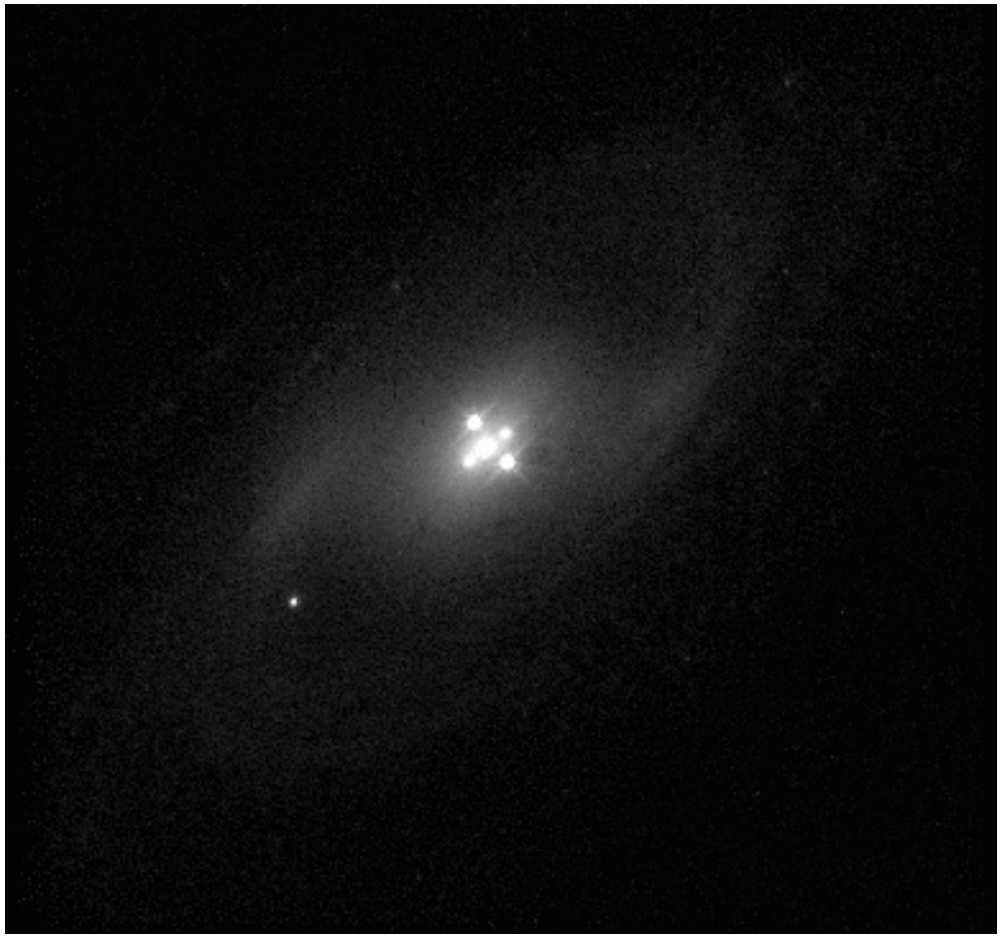

THE ASTROPHYSICAL JOURNAL, 799:149 (6pp), 2015 February 1

Jimenez-Vicente et al. 2015

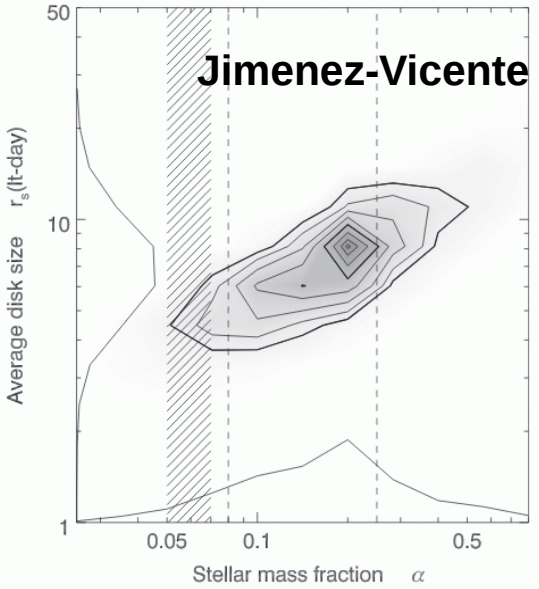

Figure 1. Likelihood function for the fraction of mass α in the form of stars or remnants, and the (Gaussian) size of the accretion disk r_s at 1736 Å (rest frame) for microlenses of mass $M = 0.3\,M_\odot$. The conto intervals of 0.25σ for one parameter from the ma and 2σ are heavier. The vertical striped band shows microlensing studies of lens samples by MED09 ar vertical dashed lines mark the region of estimates fi individual lenses (see text). The (marginalized) Ba distributions using logarithmic priors for the stellar are shown along the corresponding axis.

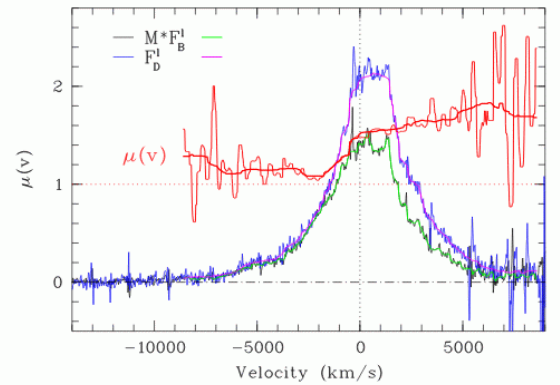

Fig. 1. Flux density ratio $\mu(v) = F^l_D/(M \times F^l_B)$ computed for the Hα emission line observed in the lensed quasar HE0435−1223. This ratio is illustrated as a function of the Doppler velocity over the useful $[-8600, 8600]\,\mathrm{km\,s^{-1}}$ velocity range (red lines). The continuum-subtracted spectra of images B and D ($M \times F^l_B$ and F^l_D, respectively) are superimposed, on an arbitrary flux scale (thin black and blue lines). These spectra were corrected for instrumental spikes and smoothed using a $220\,\mathrm{km\,s^{-1}}$ -wide median filter in the velocity range of interest (thick green and magenta lines). $\mu(v)$ is shown with the $220\,\mathrm{km\,s^{-1}}$ smoothing and a stronger one using a $1500\,\mathrm{km\,s^{-1}}$-wide median filter.

Broad emission lines are affected by microlensing different than high-ionization lines and continuum. By looking at the ratio of line vs continuum flux one can infer the amount of microlensing and constrain the amount of DM in PBHs.
Also by looking at magnification distortions within a single line

Hutsemekers et al. 2019

Very valuable tool for studying strong lenses

Particularly massive ones (clusters), where tens of background sources result in a crowded field

Take advantage of magnification boost to study fainter distant objects